Genome-Wide Association Identifies Candidate Genes for Salt Tolerance in Soybean at Emergence and Seedling Stages

Xiaojian Luo †, Yuemei Ji †, Jiangyuan Xu, Yongzhe Gu, Jun Wang, Zhangxiong Liu *, Lijuan Qiu *

Posted Date: 2 June 2026

doi: 10.20944/preprints202606.0138.v1

Keywords: soybean; salt tolerance; genome-wide association study (GWAS); candidate genes

 doi:10.20944/preprints202606.0138.v1

Article

Genome-Wide Association Identifies Candidate Genes for Salt Tolerance in Soybean at Emergence and Seedling Stages

Xiaojian Luo [1,†], Yuemei Ji [2,†], Jiangyuan Xu [1], Yongzhe Gu [1], Jun Wang [3], Zhangxiong Liu [1,*] and Lijuan Qiu [1,*]

[1] State Key Laboratory of Crop Gene Resources and Breeding/National Key Facility for Gene Resources and Genetic Improvement/Key Laboratory of Crop Germplasm Utilization, Ministry of Agriculture/Institute of Crop Sciences, Chinese Academy of Agricultural Sciences, Beijing 100081, China

[2] Institute of Crops, Ningxia Academy of Agricultural and Forestry Sciences, Yinchuan 750002, China

[3] The Shennong Laboratory, Zhengzhou 450002, China

* Correspondence: liuzhangxiong@caas.cn (Z.L.); qiulijuan@caas.cn (L.Q.)

† These authors contributed equally to this work.

Abstract

Salt stress is a primary abiotic constraint on crop production, impairing growth and reducing yield and quality in high-salinity environments. As a critical source of edible oil and protein, soybean is particularly vulnerable to salt stress during emergence and seedling establishment, making it essential to understand the genetic basis of salt tolerance at these early developmental stages for productive cultivation in saline soils. Here, a natural population of 256 soybean accessions was phenotyped for salt tolerance at emergence and seedling stages and genotyped using the ZDX1 SNP array. Genome-wide association analysis identified 60 salt tolerance-associated SNPs consolidated into 19 QTLs, 13 associated with emergence-stage and three with seedling-stage salt tolerance. Five QTLs co-localized with previously reported stress-tolerance genes, including seedling-stage QTL qSTG-SSB-03, located 192 kb from the major salt tolerance gene *GmSALT3*. Four candidate genes were prioritized: *Glyma.10G040000*, encoding a glutathione S-transferase, was identified at the emergence stage, while *Glyma.10G148700*, *Glyma.10G149200*, and *Glyma.10G149600*, encoding a calmodulin-binding protein (CaM), drought-induced protein 19 (Di19), and a protein phosphatase 2C (PP2C), respectively, were identified at the seedling stage, all with established roles in salt-stress responses.

Keywords: soybean; salt tolerance; genome-wide association study (GWAS); candidate genes

1. Introduction

Soybean (*Glycine max* [L.] Merr.) is a globally critical food and oilseed crop whose stable production underpins food security and agricultural economies worldwide [1]. Soil salinization severely constrains soybean growth, development, and yield by disrupting cellular homeostasis through ion toxicity, osmotic stress, and oxidative damage, collectively suppressing germination, root development, photosynthetic efficiency, and biomass accumulation [2,3]. Globally, an estimated 950 million hectares are affected by salinity, including roughly 20% of the 230 million hectares of irrigated land, with the affected area expanding at approximately 10% annually [4–7]. Developing salt-tolerant cultivars is consequently among the most cost-effective strategies to address this challenge [8].

Salt tolerance in soybean is a quantitative trait governed by multiple genes acting through a complex regulatory network [9]. Critically, tolerance is developmentally stage-specific: germplasm exhibiting strong tolerance at germination or seedling establishment does not necessarily perform well at maturity, and tolerance across stages can be largely uncorrelated [10–13]. Furthermore, salt

 doi:10.20944/preprints202606.0138.v1

stress during early development suppresses canopy establishment and vegetative growth, with cascading effects on subsequent stages that ultimately reduce both seed yield and protein content [14–16]. Mapping the genetic loci underlying salt tolerance specifically at emergence and seedling stages is therefore a prerequisite for breeding improved cultivars [17].

Early efforts to map soybean salt tolerance relied on biparental populations. Lee et al. [18] used an $F_{2:5}$ population from a cross between the salt-tolerant cultivar S-100 and the salt-sensitive cultivar Tokyo, mapping a major seedling-stage QTL to a 3.6 cM interval flanked by SSR markers Sat_091 and Satt237 on chromosome 3. This locus was subsequently validated across multiple studies [19–22]. In 2014, Qi et al. [23] and Guan et al. [24] independently cloned the underlying gene, *Glyma03g32900*, from wild and cultivated soybean, designating it *GmCHX1* and *GmSALT3*, respectively; the encoded cation Na^+/H^+ transporter limits Na^+ accumulation in seedling leaves, markedly improving salt tolerance. Do et al. [20] crossed salt-tolerant Fiskeby III with moderately salt-sensitive Williams 82, generating 132 F_2 families, and mapped a QTL on chromosome 13 linked to leaf sodium concentration (LSC). More recently, Li et al. [25] used a recombinant inbred line (RIL) population derived from Williams 82 × PI483460B to map *qSalt_Gm18* on chromosome 18, alongside *qSalt_Gm03*, which co-localizes with *GmCHX1* on chromosome 3. To date, 68 soybean salt tolerance QTLs identified from biparental populations have been cataloged in SoyBase (www.soybase.org).

Relative to biparental linkage mapping, genome-wide association studies (GWAS) exploit linkage disequilibrium (LD) within natural populations and offer distinct advantages: broader allelic diversity, finer mapping resolution, and no requirement to construct segregating populations [26–28]. High-density SNP-based GWAS has been widely deployed across crops, including rice [29], cowpea [30], rapeseed [31], cotton [32], alfalfa [33], and sesame [34], and has emerged as a cornerstone approach in plant molecular breeding [35]. In soybean, Kan et al. [36] applied GWAS to 191 landraces at the germination stage, identifying one significant SNP on chromosome 9 associated with the germination index ratio and seven SNPs on chromosomes 2, 3, 9, 12, and 13 associated with the germination rate ratio. Dong et al. [37] subsequently identified a major salt tolerance locus controlled by *E2*, a homolog of *Arabidopsis GIGANTEA* (*GI*), using leaf chlorosis as the phenotypic indicator; *E2* knockout enhanced tolerance by promoting peroxidase activity and reducing reactive oxygen species (ROS) accumulation under salt stress.

Despite these advances, genetic studies of salt tolerance specifically at the emergence stage remain scarce. In this study, a natural population of 256 soybean accessions was evaluated for salt tolerance at both emergence and seedling stages under controlled salt stress and genotyped with a high-density SNP array. GWAS was then conducted to identify regulatory loci and mine candidate genes, providing a resource for gene cloning and marker-assisted selection in salt-tolerance breeding programs.

2. Materials and Methods

2.1. Materials

A total of 256 soybean accessions were used in this study, comprising 255 domestic and one foreign accession (Table S1). The salt-tolerant cultivar Zhonghuang 39 and the salt-sensitive line NY27-38 served as controls throughout emergence-stage evaluations.

2.2. Salt Stress Treatment and Tolerance Assessment at the Emergence Stage

For each accession, 60 mature, uniformly sized seeds of consistent shape and color were selected. Small pots (7 × 7 × 8 cm) were filled with vermiculite to 2 cm below the rim, sown with 10 seeds each, and topped with vermiculite to the rim. Every 24 pots were arranged in a large container (46 × 32 × 10 cm). For salt treatment, 6 L of 150 mmol/L NaCl solution was added to each large container; after 5 min of saturation, the small pots were transferred to a clean container. Subsequently, 3 L of Reverse Osmosis water (RO water) was replenished every 3 days. Once the vermiculite reached its maximum water-holding capacity, the pots were immediately moved to a fresh container to prevent salt

 doi:10.20944/preprints202606.0138.v1

leaching. Control treatments were conducted identically, substituting the NaCl solution with 6 L of water. All treatments were performed in triplicate.

Emergence was scored daily from the appearance of the first seedling, defined as cotyledon protrusion above the vermiculite surface, until NY27-38 displayed clear salt-injury symptoms (severely suppressed emergence and failure of cotyledon expansion) while Zhonghuang 39 remained unaffected, with normal emergence and cotyledon expansion. At this endpoint, the number of fully established seedlings (those with expanded cotyledons and leaves) was recorded. Salt tolerance phenotypes were assessed using an individual-plant classification scheme (Figure 1; Table S2) according to Liu et al. [38], from which the salt tolerance index (SI) was calculated. Emergence-stage salt tolerance grade (STG-SI) was then assigned based on the mean SI across three replicates according to Table S2 (Figure S1). The SI was calculated as:

$$SI = \sum (I \times N_i)/10 \times 5$$

where I is the individual-plant category value, N_i is the number of plants in category I, 10 is the number of seeds sown per pot, and 5 is the maximum category value. The salt tolerance coefficient (ST) was defined as the ratio of emerged seedlings under salt stress to those under control conditions.

Figure 1. Individual-plant classification criteria for salt tolerance at the emergence stage.

2.3. Salt Stress Treatment and Tolerance Assessment at the Seedling Stage

Seed preparation and sowing for the seedling-stage assay followed the same protocol as described for the emergence stage. After sowing, 6 L of RO water was added to each large container. After 5 min of saturation, the pots were transferred to a clean container, and 3 L of RO water was replenished every 3 days using the same procedure. Once unifoliate leaves were fully expanded (approximately 10 days after sowing), salt treatment was initiated by adding 3 L of 200 mmol/L NaCl solution to each container. After saturation, pots were moved to clean containers, and this treatment was repeated on days 13 and 16. Five days after the final salt application, leaf salt-injury symptoms were scored in each replicate according to a five-grade scale (Table S3; Figure S2) following Liu [39]: grade 1, highly tolerant; grade 2, tolerant; grade 3, moderately tolerant; grade 4, sensitive; grade 5, highly sensitive. The mean grade across three replicates was calculated to assign the final seedling-stage salt tolerance grade (STG-SS), with means falling between consecutive integers rounded to the higher grade.

2.4. Phenotypic Data Processing and Analysis

Descriptive statistics and normality testing were conducted in SPSS (v25.0, IBM), and one-way ANOVA was performed in R (v4.4.2). The emergence-stage salt tolerance coefficient (ST) and salt tolerance index (SI) were standardized by rank-based inverse normal transformation (INT) following Zachary et al. [40], yielding the transformed traits ST-INT and SI-INT, respectively.

 doi:10.20944/preprints202606.0138.v1

For ordinal traits with small, skewed distributions, binarization is a recognized strategy in GWAS that sharpens contrast between phenotypic extremes and increases power to detect association signals [41], Accordingly, STG-SI and STG-SS were each binarized: accessions scoring below 3 were classified as strongly tolerant (coded 1) and those scoring 3 or above as weakly tolerant (coded 0), producing binary traits STG-SIB and STG-SSB, respectively. Pearson correlation coefficients among ST-INT, SI-INT, STG-SIB, and STG-SSB were computed using the psych package (v2.6.3) in R (v4.4.2) and visualized with the ggpairs function in the GGally package (v2.4.0).

2.5. Genotype Data Quality Control

Genomic DNA was extracted from all 256 accessions and genotyped using the ZDX1 SNP array, co-developed by the Institute of Crop Sciences, Chinese Academy of Agricultural Sciences, and Beijing Compass Biotechnology Co., Ltd. SNP quality control followed Sun et al. [42], with PLINK (v1.9) used to remove SNPs with genotype missing rate > 0.4, or minor allele frequency < 0.05.

2.6. Linkage Disequilibrium Estimation

Linkage disequilibrium (LD) decay was estimated using PopLDdecay (v3.31; BGI Genomics) and visualized in R (v4.4.2) with ggplot2 (v3.4.3). The physical distance at which r^2 declined to 0.5 (½ max r^2) was taken as the LD decay distance for this population.

2.7. Population Structure and Kinship Analysis

K-means clustering was performed using the kmeans function in R (v4.4.2), with the optimal number of subpopulations identified by the elbow method, plotting the sum of squared errors (SSE) for K = 2–10 and selecting the K at which SSE decline flattened. PCA was conducted with the prcomp function in R (v4.4.2). A neighbor-joining (NJ) phylogenetic tree was constructed from pairwise genetic distance matrices using the ape (v5.8-1) and ggtree (v3.16.0) packages. Population structure was additionally estimated with ADMIXTURE across K = 2–8, with the optimal K selected by minimizing cross-validation (CV) error. The final subpopulation assignment integrated results from K-means clustering, PCA, the NJ tree, and ADMIXTURE. A kinship matrix was computed from SNP data using GAPIT (v3.5; http://zzlab.net/GAPIT), and relatedness within and between subpopulations was visualized as a heatmap.

2.8. Genome-Wide Association Analysis (GWAS)

GWAS was conducted on the GAPIT platform (v3.5; http://zzlab.net/GAPIT) using seven models, including GLM, MLM, CMLM, MLMM, SUPER, FarmCPU, and BLINK, with population structure and kinship coefficients included as covariates to control false positives. Significant association loci were declared at a Bonferroni-corrected threshold of $-\log_{10}(P) \geq 4$, and results were visualized with ggplot2 (v3.4.3) in R (v4.4.2).

2.9. Candidate Gene Identification

LD structure around significant SNPs was examined using LDBlockShow (v1.40) to delineate haplotype blocks and identify candidate gene intervals, guided by the population's LD decay distance. Expression profiles of candidate genes across soybean tissues were retrieved from the Williams 82 reference genome on Phytozome (https://phytozome.jgi.doe.gov/pz/portal.html).

3. Results

3.1. Phenotypic Evaluation of Salt Tolerance at Emergence and Seedling Stages

At the emergence stage, the mean emergence rate under control conditions was 0.93 (range: 0.4–1.0). Salt stress reduced this significantly to a mean of 0.85 (range: 0–1.0), a difference confirmed by one-way ANOVA ($P < 0.0001$) (Figure S3).

 doi:10.20944/preprints202606.0138.v1

At the emergence stage, mean ST was 89.32 (range: 33.33–100) and mean SI was 0.62 (range: 0.09–1.00) (Table 1). Both traits deviated markedly from normality: ST was strongly left-skewed (skewness = −1.90) with a leptokurtic distribution (kurtosis = 4.60), while SI exhibited mild left skewness (skewness = −0.50). Rank-based inverse normal transformation was applied to both, and the resulting ST-INT and SI-INT closely approximated normal distributions, with skewness and kurtosis near zero, means near zero, and variance near one (Table 1; Figure S4A, B). STG-SI and STG-SS were both right-skewed (skewness = 0.52 and 0.66, respectively; Table 1) and were therefore binarized, yielding STG-SIB and STG-SSB with strongly tolerant proportions of 60.16% and 62.50%, sufficiently balanced for association analysis (Figure S4C, D). All four transformed traits were carried forward for GWAS.

Table 1. Descriptive statistics of salt tolerance at emergence and seedling stages.

Traits	Maximum	Minimum	Mean	Variance	*SD* [a]	Skewness	Kurtosis
ST [b]	100.00	33.33	89.32	128.82	11.35	-1.90	4.60
SI [c]	1.00	0.09	0.62	0.05	0.23	-0.50	-0.66
STG-SI [d]	5.00	1.00	2.43	1.30	1.14	0.52	-0.63
STG-SS [e]	5.00	1.00	2.30	1.54	1.24	0.66	-0.63
ST-INT [f]	1.34	-2.66	-0.02	0.88	0.94	-0.26	-0.57
SI-INT [g]	2.66	-2.42	0	0.96	0.98	0	-0.28
STG-SIB [h]	1.00	0	0.60	0.24	0.49	-0.41	-1.84
STG-SSB [I]	1.00	0	0.63	0.24	0.49	-0.51	-1.74

[a] *SD* is standard deviation; [b] ST is salt tolerance coefficient at emergence stage; [c] SI is salt tolerance index at emergence stage; [d] STG-SI is salt tolerance index grades at emergence stage; [e] STG-SS is salt tolerance grades at seedling stage; [f] ST-INT is salt tolerance coefficient after inverse normal transformation at emergence stage; [g] SI-INT is salt tolerance index after inverse normal transformation at emergence stage; [h] STG-SIB is salt tolerance index grades after binary conversion at emergence stage; [I] STG-SSB is salt tolerance grades following binary conversion at seedling stage.

3.2. Correlation Analysis

Pearson correlation analysis among ST-INT, SI-INT, STG-SIB, and STG-SSB revealed strong positive associations among all three emergence-stage traits (Figure 2): ST-INT vs. SI-INT, $r = 0.681$; ST-INT vs. STG-SIB, $r = 0.520$; SI-INT vs. STG-SIB, $r = 0.794$, all significant. By contrast, the seedling-stage trait STG-SSB showed negligible correlations with STG-SIB ($r = 0.062$), ST-INT ($r = 0.083$), and SI-INT ($r = 0.106$), indicating that salt tolerance at emergence and at the seedling stage are essentially independent phenotypes in this population.

ST-INT is salt tolerance coefficient after inverse normal transformation at emergence stage; SI-INT is salt tolerance index after inverse normal transformation at emergence stage; STG-SIB is salt tolerance index grades after binary conversion at emergence stage; STG-SSB is salt tolerance grades following binary conversion at seedling stage.

 doi:10.20944/preprints202606.0138.v1

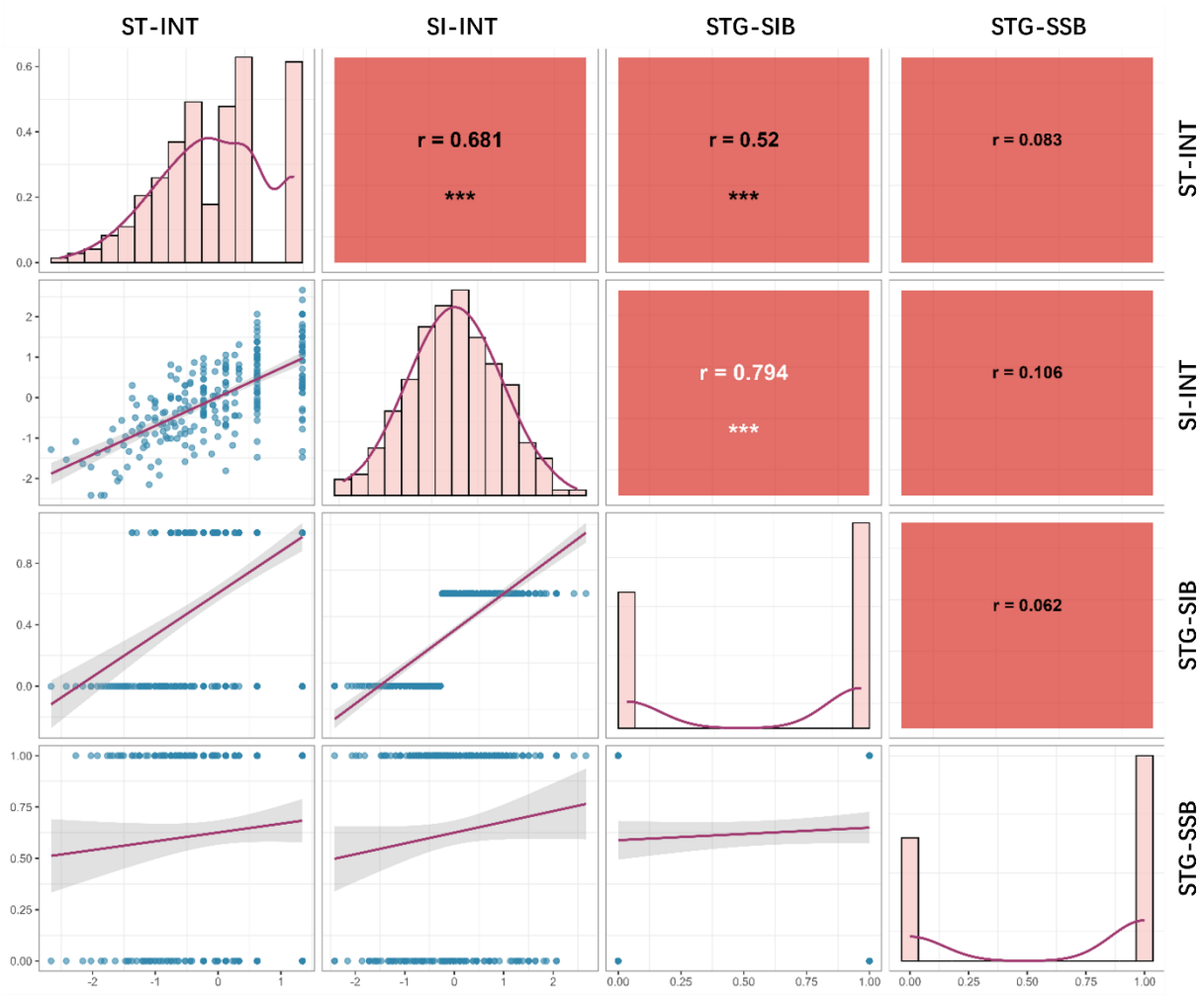

Figure 2. Phenotypic trait correlation matrix. Upper triangle: Pearson correlation coefficients with significance indicators (*P < 0.05, **P < 0.01, ***P < 0.001); diagonal: frequency distribution histograms for ST-INT, SI-INT, STG-SIB, and STG-SSB; lower triangle: scatter plots with fitted regression lines.

3.3. Genotype Data Quality Control

ZDX1 SNP array genotyping across all 256 accessions initially yielded 159,064 SNPs (Figure 3A). After PLINK-based filtering for missing rate and minor allele frequency, 89,361 SNPs were retained for GWAS.

3.4. Linkage Disequilibrium

PopLDdecay analysis showed that r^2 declined steadily with increasing physical distance, reaching the decay threshold of $r^2 = 0.5$ at approximately 50 kb (Figure 3B), which was adopted as the LD decay distance for candidate gene interval definition.

 doi:10.20944/preprints202606.0138.v1

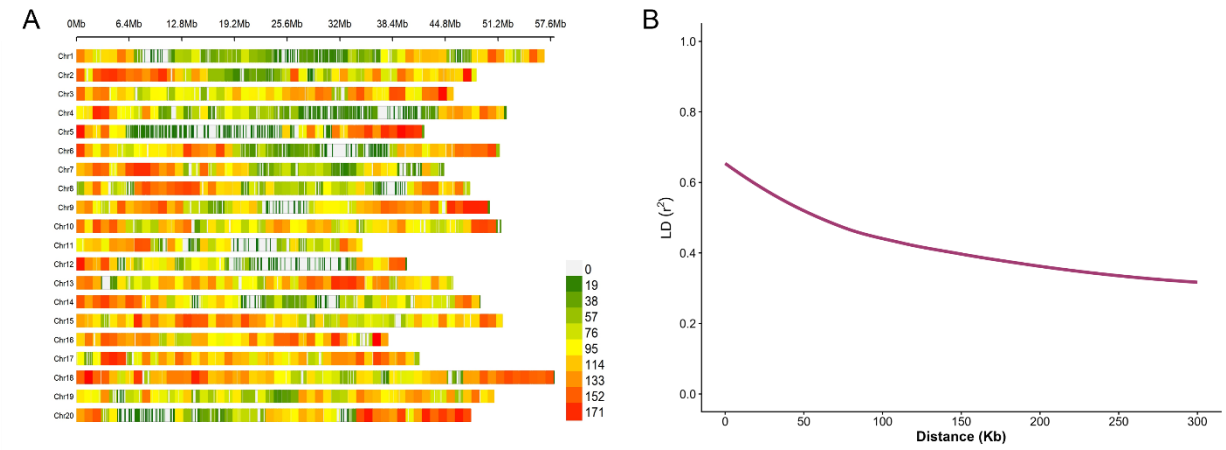

Figure 3. Genomic distribution of SNP markers and linkage disequilibrium in the 256-accession panel. (**A**) Density of the 89,361 SNPs across the 20 soybean chromosomes in 1 Mb windows; (**B**) LD decay curve showing the decline in r^2 with increasing physical distance.

3.5. Population Structure Analysis Based on Clustering, Phylogeny, and Principal Components

Four complementary methods were employed to characterize the genetic structure of this population. K-means clustering with the elbow method revealed a clear inflection point in the within-cluster sum of squares at K = 6, marking this as the most appropriate clustering solution (Figure 4A). PCA was consistent with this result, revealing pronounced genetic stratification in which PC1 and PC2 explained 13.34% and 9.84% of total genetic variation, respectively, with samples forming six discernible clusters in PC1–PC2 space (Figure 4B). NJ phylogenetic analysis independently grouped all accessions into six distinct branches (Figure 4C). ADMIXTURE analysis produced a broadly concordant outcome (Figure 4D,E): cross-validation error declined continuously with increasing K, but the per-step reduction (ΔCV) diminished progressively from K = 2 to K = 6, then rose sharply at K = 7 (ΔCV = 0.0267), pointing to six or seven as the likely range for the true number of subgroups. Integrating all four analyses, K = 6 was selected as the optimal solution for this population, with subpopulations 1 through 6 containing 15, 90, 70, 17, 22, and 35 accessions, respectively; this subpopulation assignment was incorporated into all subsequent GWAS models. The kinship heatmap further confirmed elevated relatedness among individuals within subpopulations alongside clear genetic differentiation between them (Figure 4F), a pattern consistent with within-group homogenization and between-group divergence.

 doi:10.20944/preprints202606.0138.v1

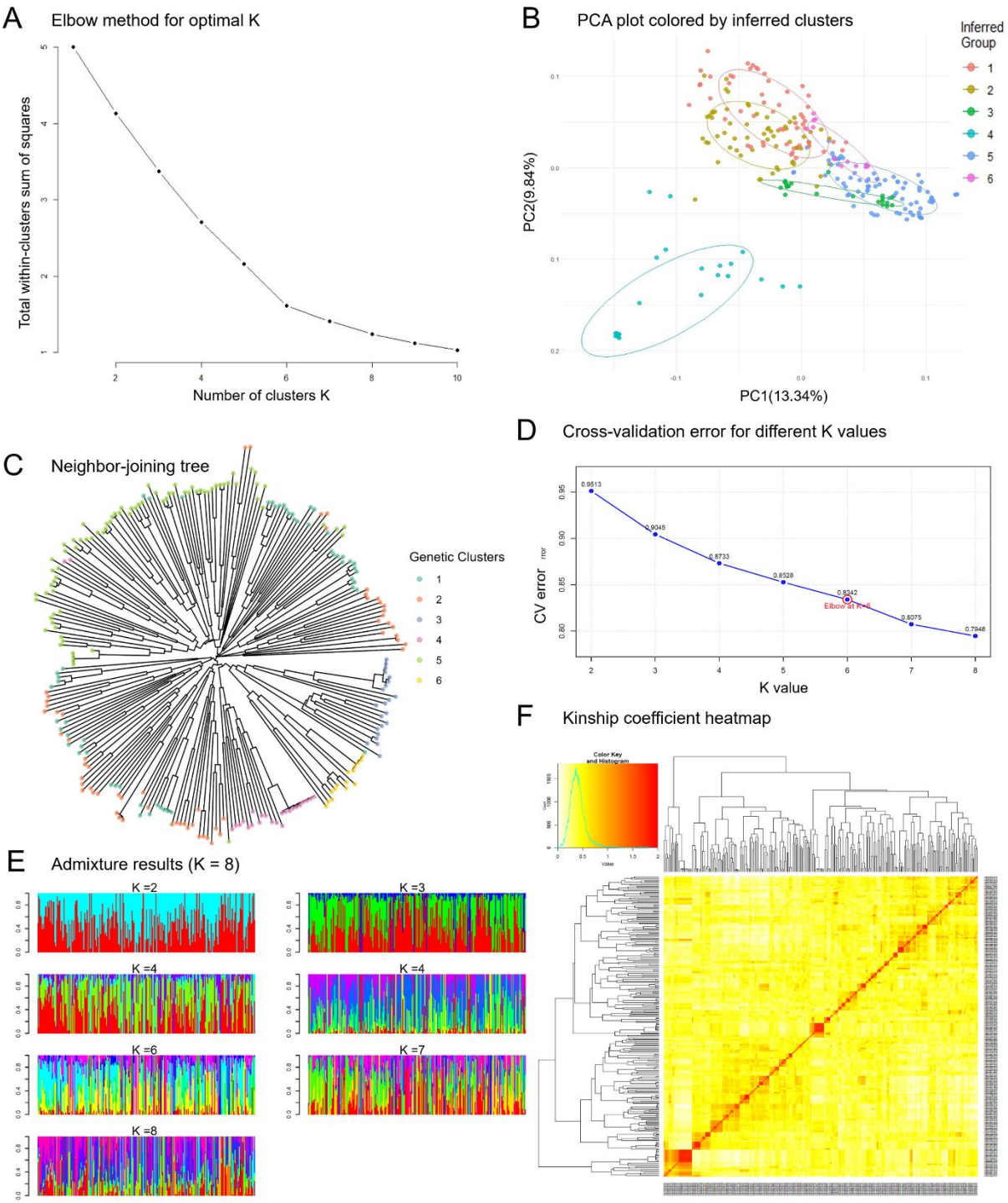

Figure 4. Genetic structure and relatedness of 256 soybean accessions. (**A**) Elbow plot from K-means clustering, used to determine the optimal number of subpopulations; (**B**) Principal component analysis scatter plot (PC1 vs. PC2) showing genetic stratification among the 256 accessions; (**C**) Neighbor-joining tree constructed using pairwise p-distances; (**D**) Cross-validation error curves across K = 2–8 used to guide ADMIXTURE model selection; (**E**) ADMIXTURE ancestry plots for K = 2–8, where each vertical bar represents one accession and colored segments denote the proportional ancestry contribution from each inferred source population; (**F**) Kinship heatmap from hierarchical clustering of all 256 accessions, with darker shading indicating closer relatedness.

3.6. Genome-Wide Association Study of Salt Tolerance-Related Traits

 doi:10.20944/preprints202606.0138.v1

GWAS was performed on the GAPIT platform for all four transformed traits, ST-INT, SI-INT, STG-SIB, and STG-SSB, using the full SNP dataset. To minimize false positives, only loci detected by at least three of the seven association models were retained. This yielded 60 significant SNPs consolidated into 19 QTLs, with the number of SNPs per QTL ranging from 1 to 20 (Table 2; Figures 5 and 6).

Three QTLs for the emergence-stage trait ST-INT were mapped to chromosomes 4, 7, and 13 (Table 2). The strongest signal was qST-INT-04 (Gm04_46793849) on chromosome 4 ($-\log_{10}P = 5.7$). The chromosome 13 locus qST-INT-13 (Gm13_35700100) was situated approximately 0.87 Mb from *GmbZIP132* [43] and 1.39 Mb from *GmBIN2* [44]. *GmbZIP132* encodes a bZIP transcription factor induced by salt and drought that positively regulates salt tolerance at seed germination [43], while *GmBIN2* encodes a GSK3-type kinase similarly induced by both stresses and a positive regulator of stress tolerance [44].

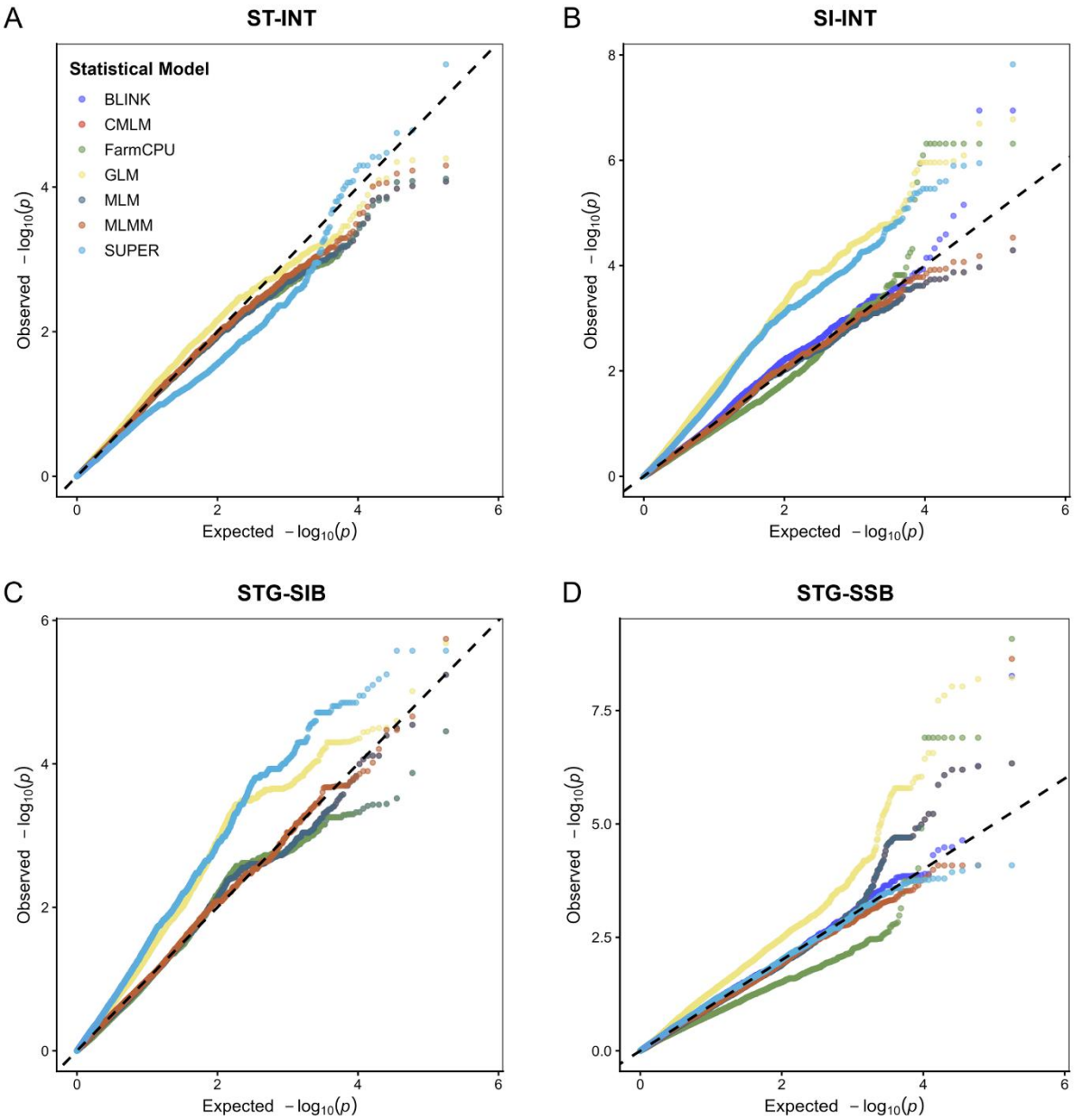

Figure 5. Quantile–quantile plots for ST-INT (**A**), SI-INT (**B**), STG-SIB (**C**), and STG-SSB (**D**) across the BLINK, CMLM, FarmCPU, GLM, MLM, MLMM, and SUPER models.

 doi:10.20944/preprints202606.0138.v1

Ten QTLs for the emergence-stage trait SI-INT were identified across chromosomes 1 (four loci), 2, 7, 9, 10, 11, and 14 (Table 2). The strongest signal came from qSI-INT-02 (Gm02_3640916–Gm02_3649811) on chromosome 2, which spanned two SNPs. The chromosome 9 locus qSI-INT-09 (Gm09_5191652) mapped approximately 1.70 Mb from *GmPHD6* [45], whose overexpression in soybean hairy roots enhances salt tolerance while knockout increases sensitivity. The chromosome 10 locus qSI-INT-10 (Gm10_3521576–Gm10_3614887) lay approximately 2.54 Mb from *GmWRKY54* [46] and 2.14 Mb from *GmERF75* [47], both implicated in salt tolerance. The chromosome 14 locus qSI-INT-14 (Gm14_6728116) was located 0.76 Mb from a previously reported marker associated with *GsPRX*, a gene involved in the oxidative stress response [48].

ST-INT is salt tolerance coefficient after inverse normal transformation at emergence stage; SI-INT is salt tolerance index after inverse normal transformation at emergence stage; STG-SIB is salt tolerance index grades after binary conversion at emergence stage; STG-SSB is salt tolerance grades following binary conversion at seedling stage.

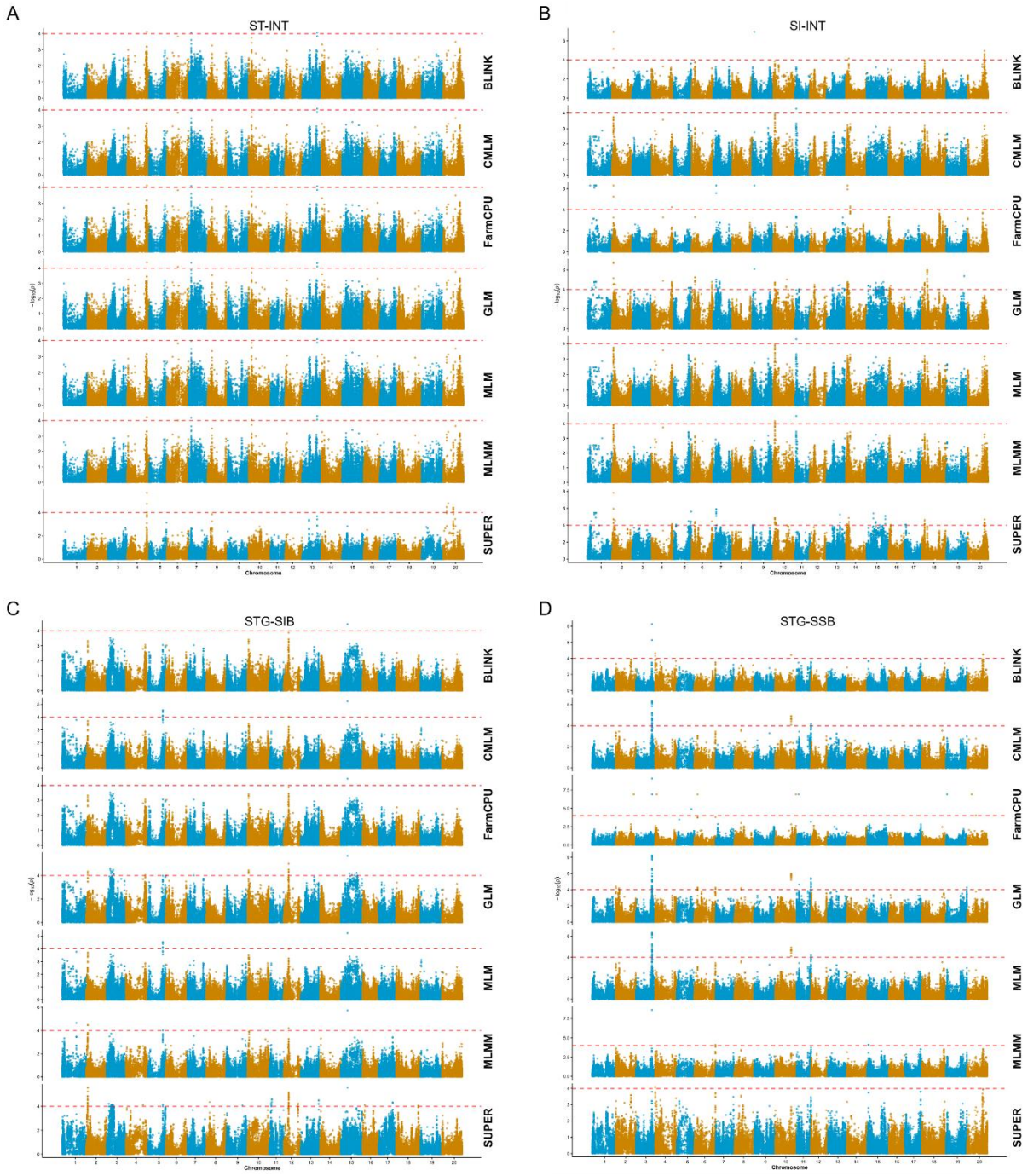

 doi:10.20944/preprints202606.0138.v1

Figure 6. Manhattan plots for ST-INT (**A**), SI-INT (**B**), STG-SIB (**C**), and STG-SSB (**D**) across the BLINK, CMLM, FarmCPU, GLM, MLM, MLMM, and SUPER models.

ST-INT is salt tolerance coefficient after inverse normal transformation at emergence stage; SI-INT is salt tolerance index after inverse normal transformation at emergence stage; STG-SIB is salt tolerance index grades after binary conversion at emergence stage; STG-SSB is salt tolerance grades following binary conversion at seedling stage.

Three QTLs for the emergence-stage binary trait STG-SIB were detected on chromosomes 5, 12, and 15 (Table 2), with qSTG-SIB-15 (Gm15_15831968) on chromosome 15 producing the strongest signal ($-\log_{10}P = 5.74$).

Three QTLs for the seedling-stage trait STG-SSB were mapped to chromosomes 3, 10, and 11 (Table 2). The chromosome 3 locus, qSTG-SSB-03 (Gm03_38525925–Gm03_38815289), was the most prominent, spanning a 0.29 Mb interval supported by 20 SNPs, with peak signal at Gm03_38688580 ($-\log_{10}P = 9.08$). This QTL lies approximately 192 kb from *Glyma03g32900* (*GmSALT3*/*GmCHX1*), the major seedling-stage salt tolerance gene cloned independently by Guan et al. [24] and Qi et al. [23], corroborating earlier reports of a major salt tolerance locus on chromosome 3 [18,21].

Table 2. Quantitative trait loci (QTL) for salt tolerance identified by GWAS in this study.

QTL name	Associated traits	Chr.	SNP interval	SNP number contained	Highest association SNP	−log10(P)
qST-INT-04	ST-INT [a]	4	Gm04_46793849	1	Gm04_46793849	5.70
qST-INT-07	ST-INT	7	Gm07_6279424	1	Gm07_6279424	4.37
qST-INT-13	ST-INT	13	Gm13_35700100	1	Gm13_35700100	4.35
qSI-INT-01-1	SI-INT [b]	1	Gm01_14874637-14927241	2	Gm01_14874637	6.09-6.32
qSI-INT-01-2	SI-INT	1	Gm01_17436477	1	Gm01_17436477	6.32
qSI-INT-01-3	SI-INT	1	Gm01_18506780	1	Gm01_18506780	6.32
qSI-INT-01-4	SI-INT	1	Gm01_19151980	1	Gm01_19151980	6.32
qSI-INT-02	SI-INT	2	Gm02_3640916-3649811	2	Gm02_3649811	6.78-7.82
qSI-INT-07	SI-INT	7	Gm07_7238076-7250804	2	Gm07_7238076	5.90-6.32
qSI-INT-09	SI-INT	9	Gm09_5191652	1	Gm09_5191652	6.95
qSI-INT-10	SI-INT	10	Gm10_3521576-3614887	3	Gm10_3521576、Gm10_3614887	4.73-4.84
qSI-INT-11	SI-INT	11	Gm11_2844635	1	Gm11_2844635	4.53
qSI-INT-14	SI-INT	14	Gm14_6728116	1	Gm14_6728116	4.86
qSTG-SIB-05	STG-SIB [c]	5	Gm05_35273972-35303385	2	Gm05_35303385	4.39-4.50
qSTG-SIB-12	STG-SIB	12	Gm12_11112335	1	Gm12_11112335	5.18
qSTG-SIB-15	STG-SIB	15	Gm15_15831968	1	Gm15_15831968	5.74
qSTG-SSB-03	STG-SSB [d]	3	Gm03_38525925-38815291	20	Gm03_38688580	4.41-9.08
qSTG-SSB-10	STG-SSB	10	Gm10_38386826-38472859	16	Gm10_38398774	5.20-6.01
qSTG-SSB-11	STG-SSB	11	Gm11_34520086-34522630	2	Gm11_34522630	4.67-4.81

[a] ST-INT is the salt tolerance coefficient after inverse normal transformation at the emergence stage; [b] SI-INT is the salt tolerance index after inverse normal transformation at the emergence stage; [c] STG-SIB is the salt tolerance index grades after binary conversion at the emergence stage; [d] STG-SSB is the salt tolerance grades after binary conversion at the seedling stage.

3.7. Candidate Gene Analysis

 doi:10.20944/preprints202606.0138.v1

To refine candidate intervals and clarify local haplotype structure, candidate gene identification focused on qSI-INT-10 (Gm10_3521576–Gm10_3614887) for emergence-stage salt tolerance and qSTG-SSB-10 (Gm10_38386826–Gm10_38472859) for seedling-stage salt tolerance, the QTLs with the greatest number of significant SNPs outside the chromosome 3 locus. LDBlockShow analysis resolved seven well-defined LD blocks (Figure S5). For qSI-INT-10, a consistent and significant LD block was detected across the GLM, MLMM, and SUPER models (Figure S5A–C), while for qSTG-SSB-10, a conserved block was identified in the BLINK, CMLM, GLM, and MLM models (Figure S5D–G).

From each stable LD block, the SNP with the highest r^2 was selected, and genes within a 50 kb window on either side were screened as candidates based on the estimated LD decay distance. Within the emergence-stage QTL qSI-INT-10, 23 candidate genes were identified (Table 3), spanning functions including cell wall biosynthesis and remodeling (e.g., cellulose synthase A4 *Glyma.10G039600* and the KATAMARI1 homolog *Glyma.10G040700*, encoding a xyloglucan galactosyltransferase), transcriptional regulation (e.g., MYB-family transcription factor APL homolog *Glyma.10G039700* and auxin response factor 1 *Glyma.10G040400*), stress response and metabolism (e.g., glutathione S-transferase *Glyma.10G040000* and alcohol dehydrogenase 1 *Glyma.10G041000*), and protein kinase activity and methylation (e.g., *Glyma.10G041300* and *Glyma.10G040100*). For the seedling-stage QTL qSTG-SSB-10, 18 candidate genes were identified (Table 3), enriched for roles in DNA metabolism and repair (e.g., RecQ family helicase *Glyma.10G148300*, Werner syndrome-like exonuclease *Glyma.10G148600*, and single-stranded DNA-binding protein *Glyma.10G149700*) and stress response (e.g., drought-induced protein 19 *Glyma.10G149200* and calmodulin-binding protein *Glyma.10G148700*), along with six uncharacterized and three functionally unknown proteins. Based on functional annotation and established relevance to salt stress, four genes, namely *Glyma.10G040000*, *Glyma.10G148700*, *Glyma.10G149200*, and *Glyma.10G149600*, were designated high-confidence candidate genes and are discussed in detail below.

Table 3. Candidate genes and functional annotations.

QTL name	Gene ID	Chr.	Start	End	Gene function
qSI-INT-10	*Glyma.10G039200*	Gm10	3476029	3482210	Tetratricopeptide repeat protein 7B-like
	Glyma.10G039300	Gm10	3484313	3487965	Rho GDP-dissociation inhibitor 1
	Glyma.10G039400	Gm10	3489552	3494424	Exocyst complex component EXO84B-like
	Glyma.10G039500	Gm10	3495933	3498821	Uncharacterized protein LOC100793067
	Glyma.10G039600	Gm10	3498156	3501931	Cellulose synthase A4
	Glyma.10G039700	Gm10	3509365	3515838	Myb family transcription factor APL-like
	Glyma.10G039800	Gm10	3523133	3524397	Unknown protein
	Glyma.10G039900	Gm10	3528125	3529563	60S ribosomal L23-like protein
	Glyma.10G040000	Gm10	3532303	3534011	Glutathione S-transferase family protein
	Glyma.10G040100	Gm10	3534381	3541727	Histone-lysine N-methyltransferase SUVR2-like
	Glyma.10G040200	Gm10	3547051	3547805	Mitochondrial import receptor subunit TOM9-2-like
	Glyma.10G040300	Gm10	3548744	3550403	Uncharacterized protein LOC102667717

 doi:10.20944/preprints202606.0138.v1

	Glyma.10G040400	Gm10	3557161	3561101	Auxin response factor 1
	Glyma.10G040500	Gm10	3561542	3565454	ATP binding/protein serine/threonine kinase
	Glyma.10G040600	Gm10	3568550	3571109	Photosystem II reaction center PSB28 protein
	Glyma.10G040700	Gm10	3572769	3575692	Xyloglucan galactosyltransferase KATAMARI1-like
	Glyma.10G040800	Gm10	3585796	3589311	Proline-rich protein precursor
	Glyma.10G040900	Gm10	3591102	3596087	Tetratricopeptide repeat protein 4 homolog
	Glyma.10G041000	Gm10	3597307	3601274	Alcohol dehydrogenase 1
	Glyma.10G041100	Gm10	3601867	3606814	3-oxoacyl-[acyl-carrier-protein] synthase
	Glyma.10G041200	Gm10	3613943	3614897	RmlC-like cupins superfamily protein
	Glyma.10G041300	Gm10	3621767	3629177	Protein kinase superfamily protein
	Glyma.10G041400	Gm10	3654431	3661105	PfkB-like carbohydrate kinase family protein
qSTG-SSB-10	*Glyma.10G148100*	Gm10	38339322	38341729	Uncharacterized protein DDB_G0271670-like
	Glyma.10G148200	Gm10	38353363	38357916	Uncharacterized protein LOC100777900
	Glyma.10G148300	Gm10	38372070	38378539	RecQ family ATP-dependent DNA helicase
	Glyma.10G148400	Gm10	38379206	38380060	Unknown protein
	Glyma.10G148500	Gm10	38381421	38382250	Protein of unknown function (DUF3511)
	Glyma.10G148600	Gm10	38382588	38389222	Werner Syndrome-like exonuclease-like
	Glyma.10G148700	Gm10	38415381	38418722	Calmodulin-binding protein
	Glyma.10G148800	Gm10	38420217	38425350	Importin subunit alpha-1b
	Glyma.10G148900	Gm10	38427372	38430979	DNA polymerase III, epsilon subunit-like protein
	Glyma.10G149000	Gm10	38431647	38436740	Syntaxin of plants 43
	Glyma.10G149100	Gm10	38441580	38441963	Unknown protein
	Glyma.10G149200	Gm10	38464899	38467826	Drought-induced 19
	Glyma.10G149300	Gm10	38468901	38469373	Uncharacterized protein LOC100797448
	Glyma.10G149400	Gm10	38469764	38473037	PHD and RING finger domain-containing protein 1
	Glyma.10G149500	Gm10	38493040	38499888	ATP binding microtubule motor family protein

 doi:10.20944/preprints202606.0138.v1

Glyma.10G149600	Gm10	38511278	38514578	Protein phosphatase 2C family protein
Glyma.10G149700	Gm10	38516493	38521186	Single-stranded DNA-binding protein
Glyma.10G149800	Gm10	38520715	38521086	Uncharacterized protein LOC102667166

4. Discussion

Salt tolerance in soybean is developmentally stage-specific [49], and tolerance at germination generally exceeds that at emergence; timely post-sowing irrigation can reduce surface salinity and partially mitigate this vulnerability [50]. In soils with dry-weight salt content below 1.0%, emergence is reduced even when germination rates remain high across genotypes. This distinction is strikingly illustrated by the cultivar Williams, which maintained a germination rate of 81% at 330 mM NaCl, yet seedling growth plummeted to just 5% under the lower concentration of 220 mM NaCl [51]. Under field conditions, seeds may germinate successfully in saline soil but fail to penetrate a salt-hardened surface crust. This demonstrates that soybean seeds can survive saline conditions during germination, while the same stress can be lethal at emergence, underscoring the need to evaluate salt tolerance, map relevant loci, and identify candidate genes specifically at the emergence stage.

Relatively few soybean salt-tolerance genes have been cloned through forward genetics to date, including the seedling-stage genes *GmSALT3*/*GmCHX1* [23,24] and *GsERD15B* [48], and the germination-stage gene *GmCDF1* [52]. The present GWAS yielded four candidate genes, one emergence-stage and three seedling-stage. The emergence-stage candidate *Glyma.10G040000*, located within qSI-INT-10, encodes a glutathione S-transferase (GST). GSTs are well-established contributors to plant salt tolerance, acting primarily by maintaining ROS homeostasis and thereby limiting salt-induced oxidative damage; transgenic overexpression of GST genes consistently enhances salt tolerance [53]. GST expression is further modulated by MYB and WRKY transcription factors, embedding these enzymes within broader stress-regulatory networks [54]. In soybean specifically, the tau-class member GmGSTU23 enhances salt tolerance through elevated glutathione transferase activity [55], suggesting that *Glyma.10G040000* may confer tolerance through analogous mechanisms centered on ROS detoxification.

The three seedling-stage candidate genes all map to qSTG-SSB-10. *Glyma.10G148700* encodes a calmodulin-binding protein, a class of regulators that decode salt-induced cytosolic Ca^{2+} transients and translate them into adaptive physiological responses. In rice, the calmodulin-binding protein OsMSR2 is strongly induced by salt stress, and its overexpression in Arabidopsis enhances tolerance by modulating ABA signaling and downstream stress-response gene expression [56]. Conversely, the *Medicago truncatula* ortholog MtCML40 acts as a negative regulator: its overexpression increases salt sensitivity, accompanied by Na^+ accumulation in shoots and suppression of the sodium efflux genes *MtHKT1;1* and *MtHKT1;2* [57]. The contrasting roles of these orthologs highlight calmodulin-binding proteins as pivotal, if context-dependent, regulators of the salt-stress response, and position *Glyma.10G148700* as a strong candidate for further functional characterization.

Glyma.10G149200 encodes drought-induced protein 19 (Di19), a family with documented roles in plant salt tolerance. In soybean, GmDi19-5 is a negative regulator that interacts with the E3 ubiquitin ligase GmPUB21 and is degraded in an ABA-dependent manner, enabling fine-tuned modulation of stress responses [58]. In maize, ZmDi19-1 enhances salt tolerance by activating downstream stress-responsive genes and boosting antioxidant capacity [59], while in cotton, GhDi19-3 and GhDi19-4 improve salt tolerance through Ca^{2+} and ABA signaling and concurrent ROS scavenging [60]. Collectively, Di19 proteins appear to function as central signaling nodes integrating multiple stress pathways, making *Glyma.10G149200* a compelling candidate for salt tolerance.

Glyma.10G149600 encodes a PP2C family protein. In Arabidopsis, PP2Cs are core negative regulators of ABA signaling and can directly interact with and inhibit the plasma membrane Na^+/H^+ antiporter SOS1, a key sodium efflux transporter [61]. In peanut, PP2C genes including *AhPP2C45*

 doi:10.20944/preprints202606.0138.v1

and *AhPP2C134* are significantly upregulated under salt stress [62]. By directly regulating sodium transport and compartmentalization, PP2Cs serve as indispensable nodes in saline-environment adaptation, supporting a role for *Glyma.10G149600* in soybean salt tolerance.

Beyond gene discovery, translating genomic findings into practical breeding requires broader consideration of how and when salt stress is evaluated. Unlike many abiotic stresses, salt-alkali stress persists throughout most or all of the crop growth cycle [63]. Current soybean salt-tolerance research is disproportionately focused on the seedling stage, under the assumption that early vegetative vigor reliably predicts agronomic performance, an assumption that does not always hold, since excessive salinity can redirect photosynthate from growth to stress tolerance. Indeed, some salt-tolerant genotypes show early vigor comparable to sensitive lines yet significantly outperform them under field conditions [50], highlighting the indispensable role of multi-stage field evaluation. Furthermore, most laboratory assays use NaCl as the sole treatment, whereas salinized soils worldwide vary widely in pH and ionic composition [64]. Salinization and alkalization frequently co-occur, yet their combined effects on plant growth are not simply additive, the severity ranking from greatest to least is saline-alkaline stress, alkaline stress, then salt stress alone, and mixed saline-alkaline injury substantially exceeds the sum of the individual stresses [65,66]. As research on mixed saline-alkaline tolerance remains sparse, future efforts should extend beyond single-salt or single-alkali treatments to encompass the complex stress combinations encountered in the field.

5. Conclusions

GWAS combining 200K SNP array data from 256 soybean germplasm accessions with salt-tolerance phenotypes at emergence and seedling stages identified 60 significant SNPs consolidated into 19 QTLs, with 13 associated with emergence-stage and three with seedling-stage salt tolerance. Known stress-tolerance genes were located near five of these QTLs; notably, the seedling-stage QTL qSTG-SSB-03 lies just 192 kb from the major salt-tolerance gene *GmSALT3*. Four high-confidence candidate genes were prioritized: the emergence-stage gene *Glyma.10G040000*, encoding a glutathione S-transferase, and the seedling-stage genes *Glyma.10G148700*, *Glyma.10G149200*, and *Glyma.10G149600*, encoding a calmodulin-binding protein, drought-induced protein 19, and a PP2C family protein, respectively. Functional validation of these candidates will be an important priority for future work.

Supplementary Materials: The following supporting information can be downloaded at the website of this paper posted on Preprints.org.

Author Contributions: Zhangxiong Liu and Lijuan Qiu: Conceptualization and writing–revision and editing. Zhangxiong Liu and Lijuan Qiu: Resources. Xiaojian Luo, Zhangxiong Liu, and Yue-mei Ji: Investigation. Xiaojian Luo, Yue-mei Ji, Jiangyuan Xu, Yongzhe Gu, and Jun Wang: Data curation and analysis. Xiaojian Luo, Zhangxiong Liu, Yue-mei Ji, Jiangyun Xu, Yongzhe Gu, and Jun Wang: Writing-original draft. For all authors: Final approval of the published version, and accountability for all aspects of the work.

Funding: This work was supported by the National Key R&D Program of China (2021YFD1201104）, the Agricultural Science and Technology Innovation Program of the Chinese Academy of Agricultural Sciences (CAAS).

Data availability statement: The data that support the findings of this study are available from the corresponding author, [ZXL], upon reasonable request.

Disclosure statement: The authors declare no potential conflicts of interest with respect to the research, authorship, and/or publication of this article.:.

References

 doi:10.20944/preprints202606.0138.v1

1. He, Y.; Chen, Y.; Yu, C.; Lu, K.; Jiang, Q.; Fu, J.; Wang, G.; Jiang, D. Photosynthesis and yield traits in different soybean lines in response to salt stress. *Photosynthetica.* 2016, 54(4), 630-635.
2. Lu, M.; Riaz, M.; Tong, K.; Hao, W.; Yang, Y.; Zhao, X.; Wang, L.; Niu, Y.; Yan, L. Boron-induced phenylpropanoid metabolism, Na^+/K^+ homeostasis and antioxidant defense mechanisms in salt-stressed soybean seedlings. *J. Hazard. Mater.* 2025, 491.
3. Singleton, P.; Bohlool, B. Effect of salinity on nodule formation by soybean. *Plant Physiol.* 1984, 74, 72-76.
4. Ajay, S. Soil salinity: a global threat to sustainable development. *Soil Use Manag*. 2022, 38, 39-67.
5. Liu, Y.; Wang, P.; Ruan, H.; Wang, T.; Yu, J.; Cheng, Y.; Kulmatoy, R. Sustainable use of groundwater resources in the transboundary aquifers of the five central Asian countries: challenges and perspectives. *Water*. 2020a, 12(8), 2101.
6. Muchate, N.; Nikalje, G.; Rajurkar, N.; Suprasanna, P.; Nikam, T. Physiological responses of the halophyte *Sesuvium portulacastrum* to salt stress and their relevance for saline soil bio-reclamation. *Flora.* 2016, 224, 96-105.
7. Radanielson, A.; Angeles, O.; Li, T.; Ismail, A.; Gaydon, D. Describing the physiological responses of different rice genotypes to salt stress using sigmoid and piecewise linear functions. *Field Crops Res.* 2018, 220, 46-56.
8. Sheng, X.; Ai, Z.; Tan, Y.; Hu, Y.; Guo, X.; Liu, X.; Sun, Z.; Yu, D.; Chen, J.; Tang, N.; et al. Novel salinity-tolerant third-generation hybrid rice developed via CRISPR/Cas9-mediated gene editing. *Int. J. Mol. Sci.* 2023, 24(9), 8025.
9. Fu, S.; Wang, L.; Li, C.; Zhao, Y.; Zhang, N.; Yan, L.; Li, C.; Niu, Y. Integrated transcriptomic, proteomic, and metabolomic analyses revealed molecular mechanism for salt resistance in soybean (*Glycine max* L.) seedlings. *Int. J. Mol. Sci.* 2024, 25(24), 13559.
10. EI-Hendawy, S.; Hu, Y.; Yakout, G.; Awad, A.; Hafiz, S.; Schmidhalter, U. Evaluating salt tolerance of wheat genotypes using multiple parameters. *Eur. J. Agron.* 2005, 22, 243-253.
11. Kingsbury, R.; Epstein, E. Selection for salt-resistant spring wheat. *Crop Sci.* 1984, 24, 310-315.
12. Manchanda, G.; Garg, N. Salinity and its effects on the functional biology of legumes. *Acta Physiol. Plant.* 2008, 30, 595-618.
13. Vicente, O.; Boscaiu, M.; Naranjo, M.; Estrelles, E.; Belles, J.; Soriano, P. Responses to salt stress in the halophyte *Plantago crassifolia* (Plantaginaceae). *J. Arid Environ.* 2004, 58, 463-481.
14. Francois, L.; Maas, E.; Donovan, T.; Youngs, V. Effect of salinity on grain-yield and quality, vegetative growth, and germination of semidwarf and durum-wheat. *Agron. J.* 1986, 78, 1053-1058.
15. Saisho, D.; Takumi, S.; Matsuoka, Y. Salt tolerance during germination and seedling growth of wild wheat *Aegilops tauschii* and its impact on the species range expansion. *Sci. Rep.* 2016, 6.
16. Shannon, M.; Grieve, C. Tolerance of vegetable crops to salinity. *Sci. Hortic.* 1999, 78, 5-38.
17. Morton, M.; Awlia, M.; Al-Tamimi, N.; Saade, S.; Pailles, Y.; Negrão, S.; Tester, M. Salt stress under the scalpel-dissecting the genetics of salt tolerance. *Plant J.* 2019, 97, 148-163.
18. Lee, G.J.; Carter, T.E.; Villagarcia, M.R.; Li, Z.; Zhou, X.; Gibbs, M.O.; Boerma, H.R. A major QTL conditioning salt tolerance in S-100 soybean and descendent cultivars. *Theor. Appl. Genet.* 2004, 109, 1610-1619.
19. Chen, H.; Cui, S.; Fu, S.; Gai, J.; Yu, D. Identification of quantitative trait loci associated with salt tolerance during seedling growth in soybean (*Glycine max* L.). *Aust. J. Agric. Res.* 2008, 59, 1086-1091.
20. Do, T.D.; Vuong, T.D.; Dunn, D.; Smothers, S.; Patil, G.; Yungbluth, D.C.; Chen, P.; Scaboo, A.; Xu, D.; Carter, T.E.; et al. Mapping and confirmation of loci for salt tolerance in a novel soybean germplasm, Fiskeby III. *Theor. Appl. Genet.* 2018,131(3), 513-524.
21. Hamwieh, A.; Tuyen, D.; Cong, H.; Benitez, E.; Takahashi, R.; Xu, D. Identification and validation of a major QTL for salt tolerance in soybean. *Euphytica.* 2011, 179, 451-459.
22. Shi, X.; Yan, L.; Yang, C.; Yan, W.; Moseley, D.O.; Wang, T.; Liu, B.; Di, R.; Chen, P.; Zhang, M. Identification of a major quantitative trait locus underlying salt tolerance in 'Jidou 12' soybean cultivar. *BMC Res. Notes.* 2018, 11, 95.
23. Qi, X.; Li, M.; Xie, M.; Liu, X.; Ni, M.; Shao, G.; Song, C.; Yim, A.K.Y.; Tao, Y.; Wong, F.L.; et al. Identification of a novel salt tolerance gene in wild soybean by whole-genome sequencing. *Nat. Commun.* 2014, 5, 4340.

 doi:10.20944/preprints202606.0138.v1

24. Guan, R.X.; Qu, Y.; Guo, Y.; Yu, L.; Liu, Y.; Jiang, J.; Chen, J.; Ren, Y.; Liu, G.; Tian, L.; et al. Salinity tolerance in soybean is modulated by natural variation in *GmSALT3*. *Plant J.* 2014, 80(6), 937-950.
25. Li, Y.; Ye, H.; Vuong, T.D.; Zhou, L.; Do, T.D.; Chhapekar, S.S.; Zhao, W.; Li, B.; Jin, T.; Gu, J.; et al. A novel natural variation in the promoter of *GmCHX1* regulates the conditional gene expression to improve salt tolerance in soybean. *J. Exp. Bot*. 2023a, 75(3), 1051-1062.
26. Hu, D.; Zhao, Y.; Zhu, L.; Li, X.; Zhang, J.; Cui, X.; Li, W.; Hao, D.; Yang, Z.; Wu, F.; et al. Genetic dissection of ten photosynthesis-related traits based on InDel-and SNP-GWAS in soybean. *Theor. Appl. Genet*. 2024, 137, 96.
27. Jang, S.; Park, S.; Lar, S.; Zhang, H.; Lee, A.; Cao, F.; Seo, J.; Ham, T.; Lee, J.; Kwon, S. Genome-wide association study (GWAS) of mesocotyl length for direct seeding in rice. *Agron.* 2021, 11, 2527.
28. Sahito, J.; Zhang, H.; Gishkori, Z.; Ma, C.; Wang, Z.; Ding, D.; Zhang, X.; Tang, J. Advancements and prospects of genome-wide association studies (GWAS) in maize. *Int. J. Mol. Sci.* 2024, 25(3), 1918.
29. Shi, H.; Zhang, W.; Cao, H.; Zhai, L.; Song, Q.; Xu, J. Identification of candidate genes for cold tolerance at seedling stage by GWAS in rice (*Oryza sativa* L.). *Biol.* 2024, 13, 784.
30. Xiong, H.; Chen, Y.; Ravelombola, W.; Mou, B.; Sun, X.; Zhang, Q.; Xiao, Y.; Tian, Y.; Luo, Q.; Alatawi, I.; et al. Genetic dissection of diverse seed coat patterns in cowpea through a comprehensive GWAS approach. *Plants.* 2024, 13, 1275.
31. Zhang, F.; Xiao, X.; Xu, K.; Cheng, X.; Xie, T.; Hu, J.; Wu, X. Genome-wide association study (GWAS) reveals genetic loci of lead (Pb) tolerance during seedling establishment in rapeseed (*Brassica napus* L.). *BMC Genom.* 2020, 21, 139.
32. Wang, L.; Yang, Y.; Qin, J.; Ma, Q.; Qiao, K.; Fan, S.; Qu, Y. Integrative GWAS and transcriptomics reveal *GhAMT2* as a key regulator of cotton resistance to *Verticillium wilt. Front. Plant Sci.* 2025, 16, 1563466.
33. He, F.; Xu, M.; Liu, H.; Xu, Y.; Long, R.; Kang, J.; Yang, Q.; Chen, L. Unveiling alfalfa root rot resistance genes through an integrative GWAS and transcriptome study. *BMC Plant Biol.* 2025, 25, 58.
34. Li, D.; Dossa, K.; Zhang, Y.; Wei, X.; Wang, L.; Zhang, Y.; Liu, A.; Zhou, R.; Zhang, X. GWAS uncovers differential genetic bases for drought and salt tolerances in sesame at the germination stage. *Genes.* 2018, 9, 87.
35. Li, B. Identification of genes conferring plant salt tolerance using GWAS: current success and perspectives. *Plant Cell Physiol*. 2020, 61(8), 1419-1426.
36. Kan, G.; Zhang, W.; Yang, W.; Ma, D.; Zhang, D.; Hao, D.; Hu, Z.; Yu, D. Association mapping of soybean seed germination under salt stress. *Mol. Genet. Genom.* 2015, 290, 2147-2162.
37. Dong, L.; Hou, Z.; Li, H.; Li, Z.; Fang, C.; Kong, L.; Li, Y.; Du, H.; Li, T.; Wang, L.; et al. Agronomical selection on loss-of-function of *GIGANTEA* simultaneously facilitates soybean salt tolerance and early maturity. *J. Integr. Plant Biol*. 2022, 64(10), 1866-1882.
38. Liu, X.X.; Chang, R.Z.; Guan, R.X.; Qiu, L.J. Establishment of salt tolerance identification method at soybean seedling emergence stage and screening of salt-tolerant germplasm. *Acta Agron. Sin*. 2020b, 46(01), 1-8.
39. Liu, X.X. Development and utilization of marker for salt-tolerant gene *GmSALT3* and identification of salt-tolerant QTL at seedling emergence stage in soybean. Master's Thesis, Chinese Academy of Agricultural Sciences, Beijing, China, 2019.
40. Zachary, R.; Jacqueline, M.; Richa, S.; Susan, R.; Lin, X. Operating characteristics of the rank-based inverse normal transformation for quantitative trait analysis in genome-wide association studies. *Biometr.* 2020, 76(4), 1262-1272.
41. Bi, W.; Zhou, W.; Zhang, P.; Sun, Y.; Yue, W.; Lee, S. Scalable mixed model methods for set-based association studies on large-scale categorical data analysis and its application to exome-sequencing data in UK Biobank. *Am. J. Hum. Genet.* 2023, 110, 762-773.
42. Sun, R.; Sun, B.; Tian, Y.; Su, S.; Zhang, Y.; Zhang, W.; Wang, J.; Yu, P.; Guo, B.; Li, H.; et al. Dissection of the practical soybean breeding pipeline by developing ZDX1, a high-throughput functional array. *Theor. Appl. Genet.* 2022, 135(4), 1413-1427.
43. Liao, Y.; Zhang, J.; Chen, S.; Zhang, W. Role of soybean *GmbZIP132* under abscisic acid and salt stresses. *Plant Physiol. Biochem.* 2008, 50(2), 221-230.

 doi:10.20944/preprints202606.0138.v1

44. Wang, L.; Chen, Q.; Xin, D.; Qi, Z.; Zhang, C.; Li, S.; Jin, Y.; Li, M.; Mei, H.; Su, A.; et al. Overexpression of *GmBIN2*, a soybean glycogen synthase kinase 3 gene, enhances tolerance to salt and drought in transgenic *Arabidopsis* and soybean hairy roots. *J. Integr. Agric.* 2018, 17(9), 1959-1971.
45. Wei, W.; Tao, J.; Chen, H.; Li, Q.; Zhang, W.; Ma, B.; Lin, Q.; Zhang, J.; Chen, S. A histone code reader and a transcriptional activator interact to regulate genes for salt tolerance. *Plant Physiol.* 2017, 175(3), 1304-1320.
46. Wei, W.; Liang, D.; Bian, X.; Shen, M.; Xiao, J.; Zhang, W.; Ma, B.; Lin, Q.; Lv, J.; Chen, X.; et al. *GmWRKY54* improves drought tolerance through activating genes in abscisic acid and Ca^{2+} signaling pathways in transgenic soybean. *Plant J.* 2019, 100(2), 384-398.
47. Zhao, M.; Yin, L.; Liu, Y.; Ma, J.; Zheng, J.; Lan, J.; Fu, J.; Chen, M.; Xu, Z.; Ma, Y. The ABA-induced soybean ERF transcription factor gene *GmERF75* plays a role in enhancing osmotic stress tolerance in *Arabidopsis* and soybean. *BMC Plant Biol.* 2019, 19(1), 1-14.
48. Jin, T.; Sun, Y.; Shan, Z.; He, J.; Wang, N.; Gai, J.; Li, Y. Natural variation in the promoter of *GsERD15B* affects salt tolerance in soybean. *Plant Biotechnol. J.* 2021, 19, 1155-1169.
49. Shelke, D.B.; Pandey, M.; Nikalje, G.C.; Zaware, B.N.; Suprasanna, P.; Nikam, T.D. Salt responsive physiological, photosynthetic and biochemical attributes at early seedling stage for screening soybean genotypes. *Plant Physiol. Biochem.* 2017, 118, 519.
50. Liu, Y.; Yu, L.L.; Qu, Y.; Chen, J.L.; Liu, X.X.; Hong, H.L.; Liu, Z.X.; Chang, R.Z.; Gilliham, M.; Qiu, L.J.; Guan, R.X. *GmSALT3*, which confers improved soybean salt tolerance in the field, increases leaf Cl^- exclusion prior to Na^+ Exclusion but does not improve early vigor under salinity. *Front. Plant Sci.* 2016, 7, 1485.
51. Hosseini, M.K.; Powell, A.A.; Bingham, I.J. Comparison of the seed germination and early seedling growth of soybean in saline conditions. *Seed Sci. Res.* 2002, 12, 165-172.
52. Zhang, W.; Liao, X.; Cui, Y.; Ma, W.; Zhang, X.; Du, H.; Ma, Y.; Ning, L.; Wang, H.; Huang, F.; et al. A cation diffusion facilitator, *GmCDF1*, negatively regulates salt tolerance in soybean. *PLoS Genet.* 2019a, 15, e1007798.
53. Meng, H.; Zhao, J.; Yang, Y.; Diao, K.; Zheng, G.; Li, T.; Dai, X.; Li, J. PeGSTU58, a glutathione s-transferase from *Populus euphratica*, enhances salt and drought stress tolerance in transgenic *Arabidopsis*. *Int. J. Mol. Sci.* 2023, 24(11), 9354.
54. Yuan, L.; Dang, J.; Zhang, J.; Wang, L.; Zheng, H.; Li, G.; Li, J.; Zhou, F.; Khan, A.; Zhang, Z.; et al. A glutathione S-transferase regulates lignin biosynthesis and enhances salt tolerance in tomato. *Plant Physiol.* 2024, 196(4), 2989-3006.
55. Li, X.; Pang, Y.; Zhong, Y.; Cai, Z.; Ma, Q.; Wen, K.; Nian, H. *GmGSTU23* encoding a tau class glutathione s-transferase protein enhances the salt tolerance of soybean (*Glycine max* L.). *Int. J. Mol. Sci.* 2023b, 24(6), 5547.
56. Xu, G.; Rocha, P.; Wang, M.; Xu, M.; Cui, Y.; Li, L.; Zhu, Y.; Xia, X. A novel rice calmodulin-like gene, *OsMSR2*, enhances drought and salt tolerance and increases ABA sensitivity in *Arabidopsis*. *Plant.* 2022, 234, 47-59.
57. Zhang, X.; Wang, T.; Liu, M.; Sun, W.; Zhang, W. Calmodulin-like gene *MtCML40* is involved in salt tolerance by regulating MtHKTs transporters in *Medicago truncatula*. *Environ. Exp. Bot.* 2019b, 157, 79-90.
58. Yang, Y.; Ren, R.; Karthikeyan, A.; Yin, J.; Jin, T.; Fang, F.; Cai, H.; Liu, M.; Wang, D.; Zhi, H.; et al. The soybean GmPUB21-interacting protein GmDi19-5 responds to drought and salinity stresses via an ABA-dependent pathway. *Crop J.* 2023, 11(4), 1152-1162.
59. Zhang, X.; Cai, H.; Lu, M.; Wei, Q.; Xu, L.; Bo, C.; Ma, Q.; Zhao, Y.; Cheng, B. A maize stress-responsive Di19 transcription factor, *ZmDi19-1*, confers enhanced tolerance to salt in transgenic *Arabidopsis*. *Plant Cell Rep.* 2019c, 38, 1563-1578.
60. Zhao, L.; Li, Y.; Li, Y.; Chen, W.; Yao, J.; Fang, S.; Lv, Y.; Zhang, Y.; Zhu, S. Systematical characterization of the cotton *Di19* gene family and the role of *GhDi19-3* and *GhDi19-4* as two negative regulators in response to salt stress. *Antioxidants.* 2022, 11(11), 2225.
61. Fu, H.; Yu, X.; Jiang, Y.; Wang, Y.; Yang, Y.; Chen, S.; Chen, Q.; Guo, Y. SALT OVERLY SENSITIVE 1 is inhibited by clade D Protein phosphatase 2C D6 and D7 in *Arabidopsis thaliana*. *Plant Cell*. 2023, 35(1), 279-297.

 doi:10.20944/preprints202606.0138.v1

62. Wu, Z.; Luo, L.; Wan, Y.; Liu, F. Genome-wide characterization of the *PP2C* gene family in peanut (*Arachis hypogaea* L.) and the identification of candidate genes involved in salinity-stress response. *Front. Plant Sci.* 2023, 14, 1093913.
63. Ha, B.K.; Vuong, T.D.; Velusamy, V.; Nguyen, H.T.; Shannon, J.G.; Lee, J.D. Genetic mapping of quantitative trait loci conditioning salt tolerance in wild soybean (*Glycine soja*) PI 483463. *Euphytica.* 2013, 193(1), 79-88.
64. Rengasamy, P. Soil processes affecting crop production in salt-affected soils. *Funct. Plant Biol.* 2010, 37(7), 613-620.
65. Gong, B.; Wang, X.F.; Wei, M.; Li, Y.; Shi, Q.H. Overexpression of *S-adenosylmethionine synthetase 1* enhances tomato callus tolerance to alkali stress through polyamine and hydrogen peroxide cross-linked networks. *Plant Cell Tissue Organ Cult.* 2016, 124(2), 377-391.
66. Wang, X.P.; Jiang, P.; Ma, Y.; Geng, S.J.; Wang, S.C.; Shi, D.C. Physiological strategies of sunflower exposed to salt or alkali stresses: restriction of ion transport in the cotyledon node zone and solute accumulation. *Agron. J.* 2015, 107(6), 2181-2192.